Published in GNSS 17th International Technical Meeting of the Satellite Division, 2458-2467, 2004
which should be used for any reference to this work

Performance Analysis of Mobile Station Location Using Hybrid GNSS and Cellular Network Measurements

Cyril Botteron, Elham Firouzi, Pierre-André Farine
Institute of Microtechnology, University of Neuchâtel, Neuchâtel, Switzerland

BIOGRAPHIES

Dr. Cyril Botteron is maître assistant (assistant professor) at the Institute of Microtechnology, University of Neuchâtel, Switzerland. He received his Ph.D. in Electrical Engineering from the University of Calgary, Canada. His current research interests comprise the development of radio frequency (RF) integrated circuits and statistical signal processing techniques with applications in digital and wireless communications, including global navigation satellite systems (GNSS) and ultra-wideband (UWB) communications.

Dr. Elham Firouzi is maître assistant (assistant professor) at the Institute of Microtechnology, University of Neuchatel, Switzerland. He received his Ph.D. in 1995. Currently, he is leading a project in the domain of GPS timing, which is realized in collaboration with local industry.

Dr. Pierre-André Farine is professor of electronics and signal processing at the Institute of Microtechnology IMT, University of Neuchâtel, Switzerland. He works in the field of low-power integrated products for portable devices, including wireless telecommunication and GNSS systems. He is Head of the electronics and signal processing laboratory (ESPLAB) at IMT. His R&D group works also for video and audio compression algorithms and signal processing. He received his Doctoral and MSc Degree from University of Neuchâtel. He was working 17 years for Swiss watch industries (Swatch Group), including developments for high-tech products, such as wrist-watch cellular phones and GPS watch prototypes.

ABSTRACT

Recently, different hybrid GNSS/cellular methods combining GNSS measurements with cellular network measurements have been proposed. These methods are designed to improve the availability (and accuracy) of position determination in situations where few satellite signals can be received, such as in urban canyons or even indoor environments.

In order to get some interesting insights into the performance of these hybrid GNSS/cellular methods under various conditions and system geometry configurations, we present in this paper a detailed analytical and numerical performance analysis. Our analysis is based on the Cramer-Rao lower bound (CRLB) theory for deterministic and random parameters, as well as an analytical asymptotic expression for the location mean-square error (MSE).

Based on this theoretical framework, we investigate analytically and using Monte-Carlo simulations how the positioning accuracy of different hybrid systems is affected by the relative geometry and the type and number of measurements between the mobile station (MS), the cellular base stations (BSs), and the satellites. The effect of important biased cellular network measurement errors (such as due to multipath and non line of sight (NLOS) propagation) are also considered.

INTRODUCTION

With the convergence of wireless communications and positioning technologies, a plethora of new services will originate, such as for location-based emergency services (E-911), personal security and safety, traffic monitoring, fleet and asset tracking, and wireless internet services.

While the cellular network infrastructure can be used to provide a position estimate of the MS, based on a combination of signal parameter measurements (e.g., round-trip delay (RTD) or time difference of arrivals (TDOA)), the positioning accuracy is often very limited in urban environments due to important multipath and NLOS effects that result in important biased measurements. Moreover, in rural environments where only few cellular BSs are available, the minimum number of BSs necessary to estimate the position of the MS (e.g., by trilateration) may not always be sufficient. On the other hand, a GNSS receiver or assisted-GNSS receiver embedded in a MS handset can provide accurate positioning results in open sky conditions, but the performance may deteriorate seriously in urban canyons where the geometrical dilution of precision (GDOP) can be relatively large (clustered satellites at high elevation angles) and/or the number of satellites may not be sufficient to provide a determined solution.

Consequently, in the near future, hybrid approaches combining cellular network measurements and assisted GNSS measurements will likely provide the best accuracy and positioning availability. However, only some preliminary results on hybrid GNSS/cellular systems have been published so far (see, e.g., [1], [2], [3], [4]). In this paper, we thus present some interesting insights into the contribution to accuracy of different type of measurements (e.g., range vs. pseudo-range measurements) and data aiding information (e.g., altitude and time aiding information), under various conditions and assumptions (e.g., for different number of satellites and BSs, for GNSS time synchronized and non-synchronized BSs, etc.). Our approach is based on the CRLB theory for deterministic and random parameters as well as an asymptotic MSE analysis used to assess the effects of biased measurements on the positioning accuracy.

SYSTEM MODEL DEFINITIONS AND ASSUMPTIONS

We consider a hybrid GNSS/cellular system exploiting various range and/or pseudo-range measurements made with respect to several satellite and cellular BS positions. For mathematical simplicity, we use a local level frame $[x, y, z]^T$ centered on the MS or user position $\mathbf{u} = [u_x, u_y, u_z]^T$ (see Fig. 1), and assume that the satellite and user's coordinates are fixed.

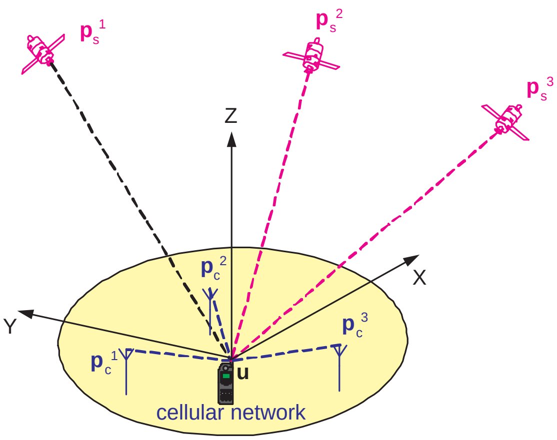

Fig. 1 Example of hybrid GNSS/cellular system geometry.

We denote the position of the satellite i as $\mathbf{p}_s^i = [p_{s,x}^i, p_{s,y}^i, p_{s,z}^i]^T$, the cellular base station j as $\mathbf{p}_c^j = [p_{c,x}^j, p_{c,y}^j, p_{c,z}^j]^T$, and the GNSS clock bias as t_s.

We write the ith pseudo-range measurement between the MS and the satellite or cellular base station position $\mathbf{p}_v^i$, $v \in \{s, c\}$ as

$$\eta_i = \|\mathbf{p}_v^i - \mathbf{u}\| + t_s + \epsilon_i \quad (1)$$

where ϵ_i is some random error (e.g., including multipath component, satellite or cellular's clock error, satellite's inonospheric and tropospheric propagation delays) and for mathematical simplicity η_i and ϵ_i are expressed in the same unit as the positions, i.e., in meters (t_s is obtained by multiplying the actual clock bias in seconds with the speed of light or approximately $3 \times 10^8\ m/s$).

Finally, we define a M-dimensional measurement vector $\boldsymbol{\eta} = [\eta_1, \eta_2, ..., \eta_M]$ containing the pseudo-range and/or range measurements from the satellites and/or terrestrial base stations and a 4-dimensional estimation vector $\mathbf{x}$ containing the unknown MS's position and clock offset to be estimated, i.e., $\mathbf{x} = [\mathbf{u}, t_s]$.

In the following, we always assume that at least 4 hybrid measurements are available so that a bound on the estimation error can be calculated. Furthermore, when the minimum number of measurements leads to an ambiguity between two possible solutions for the MS's position, we assume that the correct one is selected using some a-priori information (solution ambiguities are not reflected in the bounds calculations). The different hybrid GNSS/cellular cases we consider are:

C1) *3 SAT*$_{3PR}$ *+ 1 BS*$_{PR}$*:* the cellular BSs are GNSS time synchronized and the number of satellite and cellular pseudo-range (PR) measurements is 3 and 1, respectively.

C2) *3 SAT*$_{3PR}$ *+ 1 BS*$_{RTD+PR}$*:* in addition to 3 satellites and one cellular pseudo-range measurements, a RTD between one GNSS time-synchronized BS and the MS is used as time aiding information to adjust the MS's time reference to correspond to ”true” GNSS time (i.e., the MS uses the RTD measurement together with the transmitted BS's GNSS time to adjust its time reference). As compared to case C1, the addition of this time aiding information leads to an over-determined system of equations.

C3) *3 SAT*$_{3PR}$ *+ 1 BS*$_{RTD}$*:* in addition to 3 satellite pseudo-range measurements, a RTD between one GNSS time-synchronized BS and the MS is used as time aiding information.

C4) *3 SAT*$_{3PR}$ *+ 1BS*$_{ALT}$*:* the MS uses altitude (ALT) aiding information (delivered from one BS) in addition to 3 GNSS pseudo-range measurements.

C5) *3 SAT*$_{3PR}$ *+ 1BS*$_{RTD+ALT}$*:* the MS uses both time and altitude aiding information (delivered from one GNSS time-synchronized BS) in addition to 3 GNSS measurements, leading to an over-determined system of equations.

C6) *4 SAT*$_{4PR}$*:* the MS only uses 4 GNSS pseudo-range measurements (this case, which is not a hybrid case, will be considered as a reference for performance evaluation).

C7) *2 SAT*$_{2PR}$ *+ 2 BS*$_{2PR}$*:* the cellular BSs are GNSS time synchronized and the number of satellite and cellular pseudo-range measurements is 2.

C8) *2 SAT*$_{2PR}$ *+ 2 BS*$_{RTD+2PR}$*:* the cellular BSs are GNSS time synchronized and the MS uses time aiding information in addition to 2 GNSS and 2 cellular pseudo-range measurements, leading to an over-determined system of equations.

C9) *2 SAT$_{2PR}$ + 1 BS$_{RTD+ALT}$:* the MS uses both time and altitude aiding information (delivered from one GNSS time-synchronized BS) in addition to two satellite pseudo-range measurements.

C10) *1 SAT$_{PR}$ + 3 BS$_{3PR}$:* the cellular BSs are GNSS time synchronized and the number of satellite and cellular pseudo-range measurements is 1 and 3, respectively.

C11) *1 SAT$_{PR}$ + 3 BS$_{RTD+3PR}$:* the cellular BSs are GNSS time synchronized and the MS uses time aiding information in addition to 1 GNSS and 3 cellular pseudo-range measurements (leading to an over-determined system of equations).

LOCATION PERFORMANCE BENCHMARKS

We now present and discuss different benchmarks that can be used to assess the performance of different hybrid GNSS/cellular systems (including but not limited to the hybrid cases discussed above).

Cramer-Rao lower bound

Because the CRLB provides a lower limit for the minimal achievable variance for any unbiased estimator, it is an important benchmark (it should be noted that the CRLB can be reached for sufficiently large sample size by the maximum likelihood estimator (MLE), which is asymptotically efficient)

Assuming that the the error term ϵ_i in the pseudo-range measurement equation (1) can be modelled as a zero-mean independent Gaussian distributed random variable with covariance matrix $\mathbf{Q}$, i.e., $pr(\boldsymbol{\eta}|\mathbf{x}) \sim N[f(\mathbf{x}), \mathbf{Q}]$, the CRLB matrix for $\mathbf{x}$ can be expressed under standard regularity conditions as the inverse of the Fisher information matrix (FIM) $\mathbf{J}(\mathbf{x})$ (see, e.g., [5, 6]), i.e.,

$$\mathbf{J}(\mathbf{x}) = -E_\eta \left[\frac{\partial}{\partial \mathbf{x}} \left(\frac{\partial}{\partial \mathbf{x}} \ln pr(\boldsymbol{\eta}|\mathbf{x}) \right)^T \right]. \qquad (2)$$

where E_η denotes statistical expectation over $\boldsymbol{\eta}$, and the derivatives are evaluated at the true values of $\mathbf{x}$.

Using (1) and (2), it is easy to show that the CRLB for $\mathbf{x}$ can be written as (see, e.g., [7, 8, 9, 10])

$$\mathrm{CRLB}(\mathbf{x}) \stackrel{\mathrm{def}}{=} J^{-1}(\mathbf{x}) = \left(\mathbf{H}\mathbf{Q}^{-1}\mathbf{H}^T \right)^{-1} \qquad (3)$$

where $\mathbf{H}$ is a transformation matrix whose elements are defined as

$$(\mathbf{H})(i,j) = \{\partial \eta_j / \partial x_i\}. \qquad (4)$$

Observation 1 *We note that (3) only holds for Gaussian distributed pseudo-range measurements, which is a relatively strong assumption given that the pseudo-range measurements can not (in general) be expressed as a linear function of the received signal samples at the antenna receiver. Thus, even if the signal samples at the MS's receiving antenna are assumed statistically Gaussian distributed (which is justified in practice based on thermal noise considerations), the pseudo-range measurements should not be expected to be Gaussian distributed. However, in [11], it was shown that by assuming a specular multipath environment and a vector* $\mathbf{s}$ *of independent Gaussian distributed signal samples at the antenna receivers (which is a more realistic assumption), i.e.,* $pr(\mathbf{s}|\breve{\boldsymbol{\eta}}) \sim N[g(\breve{\boldsymbol{\eta}}), \mathbf{C}_s]$*, where* $\breve{\boldsymbol{\eta}}$ *contains both the LOS and the NLOS signal parameters, the CRLB for* $\mathbf{x}$ *could also be expressed as a function of the CRLB for a parameter vector* $\boldsymbol{\eta} \subseteq \breve{\boldsymbol{\eta}}$ *containing the parameters actually used to estimate* $\mathbf{x}$ *(such as the LOS pseudo-ranges) and estimated at the MS and/or at the BSs, i.e., as*

$$\tilde{\mathrm{CRLB}}(\mathbf{x}) \stackrel{\mathrm{def}}{=} \tilde{J}^{-1}(\mathbf{x}) = \left(\mathbf{H}\{\mathrm{CRLB}(\boldsymbol{\eta})\}^{-1}\mathbf{H}^T \right)^{-1} \qquad (5)$$

where $\mathrm{CRLB}(\boldsymbol{\eta})$ *is the matrix obtained by deleting the rows and columns of* $\breve{\mathrm{CRLB}}(\breve{\boldsymbol{\eta}})$ *that correspond to the subset of parameters that are not used by the positioning system to estimate* $\mathbf{x}$ *(such as the NLOS signal measurements),* $\mathbf{H}$ *is defined as* $(\mathbf{H})(i,j) = \{\partial \eta_j / \partial x_i\}$*, and* $\breve{\mathrm{CRLB}}(\breve{\boldsymbol{\eta}})$ *is calculated (under standard regularity conditions) as the inverse of the FIM* $\breve{\mathbf{J}}(\breve{\boldsymbol{\eta}})$*, i.e., as*

$$\breve{\mathbf{J}}(\breve{\boldsymbol{\eta}}) = -E_s \left[\frac{\partial}{\partial \breve{\boldsymbol{\eta}}} \left(\frac{\partial}{\partial \breve{\boldsymbol{\eta}}} \ln pr(\mathbf{s}|\breve{\boldsymbol{\eta}}) \right)^T \right]. \qquad (6)$$

Observation 2 *by noting that (5) (which assumes the joint use of all the signal samples received at possibly* C *different physical locations to estimate* $\mathbf{x}$*) has the same functional form as the location CRLB (3) (which assumes the use of an unbiased and Gaussian distributed signal measurement vector* $\boldsymbol{\eta}$ *with covariance matrix* $\mathbf{Q}$ *to estimate* $\mathbf{x}$*), we can infer the following: if an unbiased and efficient estimator for the signal measurements in* $\boldsymbol{\eta}$ *exists, i.e., an unbiased estimator* $\hat{\boldsymbol{\eta}} = [\hat{\boldsymbol{\eta}}_1^T, \cdots, \hat{\boldsymbol{\eta}}_C^T]^T$*, where* $\hat{\boldsymbol{\eta}}_c$ *estimated at the* c*th MS or BS receiver position can reach* $\mathrm{CRLB}(\boldsymbol{\eta}_c)$ *for* $c = 1, \cdots, C$ *(i.e., if we can write* $\mathbf{Q} = \mathrm{diag}\{\mathrm{CRLB}(\boldsymbol{\eta}_1), \cdots, \mathrm{CRLB}(\boldsymbol{\eta}_C)\}$*), then any unbiased position estimator using jointly these signal measurements will also be bounded by (5), the same lower bound as for an optimal position estimator using jointly all of the information in the received signal samples at* C *FSs.*

This observation is very important for a hybrid GNSS/cellular system since the signal samples are often received at different physical locations (e.g., at the MS for the satellite signals and at the BSs for the cellular signals), and it is much easier and practical to transmit to the MS the BSs' signal measurements (e.g., the RTDs, the PRs) rather than all the received signal samples. Note that while the same observation could have been obtained by observing that the signal measurements in $\boldsymbol{\eta}$ *or* $\breve{\boldsymbol{\eta}}$ *are a sufficient statistic for the MS's position vector* $\mathbf{x}$*, it does not seem possible to prove that* $\boldsymbol{\eta}$ *or* $\breve{\boldsymbol{\eta}}$ *is a sufficient statistic for* $\mathbf{x}$ *because of the complicated mathematical expression for the probability density function (p.d.f.)* $pr(\mathbf{s}|\breve{\boldsymbol{\eta}})$ *or* $pr(\mathbf{s}|\boldsymbol{\eta})$ *for the signal parameters in a general specular multipath environment.*

Observation 3 *since the above CRLB derivations do not assume a particular multilateration technique (e.g., circular,* *hyperbolic, or elliptical trilateration) and multisensor data fusion method, the CRLB formulas (3) and (5) can be used to bound the position estimation variance for any unbiased multilateral radio location estimators.*

Extension of the CRLB in the presence of random parameter measurements

As discussed above, altitude aiding (see hybrid case C4) and/or time aiding (see hybrid case C3) from a cellular BS can be used to set (or program) the MS's receiver altitude or GNSS time, respectively. In this case, the MS's altitude and/or GPS time offset are better modelled as random quantities rather than deterministic quantities (due to estimation errors, their mean is assumed deterministic, but their error is random with a given p.d.f.). For these hybrid cases, we thus assume that the estimation vector $\mathbf{x}$ is composed of both deterministic (the MS's horizontal (and vertical) cartesian coordinates) and random (the clock bias t_s and/or the altitude u_z) quantities, and we compute the FIM for $\mathbf{x} = [\mathbf{u}, t_s]$ as [6]

$$\mathrm{CRLB}_T^{-1}(\mathbf{x}) \stackrel{\mathrm{def}}{=} \mathbf{J}_T(\mathbf{x}) = \mathbf{J}_D(\mathbf{x}) + \mathbf{J}_P(\mathbf{x}) \tag{7}$$

where $\mathbf{J}_D(\mathbf{x})$ represents information obtained from the signal measurements and is obtained as the statistical expectation taken over the random parameter(s) of $\mathbf{J}(\mathbf{x})$, i.e., $\mathbf{J}_D(\mathbf{x}) = E_x[\mathbf{J}(\mathbf{x})]$ (see (3), (5) for expressions for $\mathbf{J}(\mathbf{x})$), and $\mathbf{J}_P(\mathbf{x})$ represents the a priori information and is given by

$$\mathbf{J}_P(\mathbf{x}) = -E_x\left[\frac{\partial}{\partial \mathbf{x}}\left(\frac{\partial}{\partial \mathbf{x}} \ln pr(\mathbf{x})\right)^T\right].$$

Observation 4 *Note that $\mathbf{J}_D(\mathbf{x})$ and $\mathbf{J}_P(\mathbf{x})$ do not need to be non-singular for $\mathbf{J}_T(\mathbf{x})$ to be non-singular. For example, assuming as time aiding information that the clock bias t_s is distributed as $t_s \sim N[\bar{t}_s, \sigma_{t_s}^2]$, then $\mathbf{x} = [\mathbf{u}, t_s]$ and with only 3 pseudo-range measurements $\mathbf{J}_D(\mathbf{x})$ and $\mathbf{J}_P(\mathbf{x})$ will be singular while $\mathbf{J}_T(\mathbf{x}) = \mathbf{J}_D(\mathbf{x}) + \mathbf{J}_P(\mathbf{x})$ will not in general (unless a bad geometry is assumed, e.g., co-located satellites or BSs).*

*E*xpressions for $\mathbf{J}_D(\mathbf{x})$ and $\mathbf{J}_P(\mathbf{x})$ for the hybrid cases C2-C5, C8-C9, and C11:

With altitude aiding information, we model the altitude as a normal random variable with mean $\bar{u}_z$ and variance $\sigma_{u_z}^2$ (i.e., we assume that the MS can be located below or above an average altitude $\bar{u}_z$, stored at the BS). Thus, the 4×4 matrix $\mathbf{J}_P(\mathbf{x})$ for the hybrid case C4 becomes

$$\mathbf{J}_P(\mathbf{x}) = \mathrm{diag}\{0, 0, 1/\sigma_{u_z}^2, 0\}. \tag{8}$$

With RTD-based time aiding information, we model t_s as a normal random variable with mean $\bar{t}_s$ and variance $\sigma_{t_s}^2$, i.e., as $t_s \sim N[\bar{t}_s, \sigma_{t_s}^2]$ (NLOS propagation does not impact the estimation of the GNSS clock time t_s at the MS, given reciprocity of propagation times on the forward and reverse link [4]). Thus, for the hybrid cases C2-C3, C8 and C11, the matrix $\mathbf{J}_P(\mathbf{x})$ is

$$\mathbf{J}_P(\mathbf{x}) = \mathrm{diag}\{0, 0, 0, 1/\sigma_{t_s}^2\} \tag{9}$$

while for the hybrid cases C5 and C9, it is

$$\mathbf{J}_P(\mathbf{x}) = \mathrm{diag}\{0, 0, 1/\sigma_{u_z}^2, 1/\sigma_{t_s}^2\}. \tag{10}$$

For the matrix $\mathbf{J}_D(\mathbf{x})$, we need to calculate $\mathbf{J}_D(\mathbf{x}) = E_x[\mathbf{J}(\mathbf{x})]$. For the hybrid cases C2-C3, C8 and C11, we obtain readily that $\mathbf{J}_D(\mathbf{x}) = \mathbf{J}(\mathbf{x})$ since $\mathbf{J}(\mathbf{x})$ does not contain t_s, while for the other cases, we have $\mathbf{J}_D(\mathbf{x}) = E_{u_z}[\mathbf{J}(\mathbf{x})] \approx \mathbf{J}(\mathbf{x})$ since the variation in satellite's azimuth and elevation due to a small change in the MS's altitude is negligible.

Asymptotic MSE expression in the presence of biased measurements

Until now, we have assumed unbiased pseudo-range measurements and derived the CRLB for any unbiased estimator of $\mathbf{x}$. Unfortunately, it is not always possible to make unbiased measurements (especially for the low elevation cellular signals) and a more realistic model than (1) for the ith pseudo-range measurement η_i is

$$\eta_i = \|\mathbf{p}_v^j - \mathbf{u}\| + t_s + b_i + \epsilon_i \,,\, v \in \{s, c\} \tag{11}$$

where b_i is some unknown deterministic measurement bias for the ith measurement. While this bias can in general be neglected for LOS satellite measurements, it can be used to model the NLOS and multipath effects of cellular measurements which can be very important in urban or suburban areas due to numerous man-made or natural obstructions of the LOS paths. Note that practically, the time bias b_i may be time varying over a long time interval. However, we can justify the deterministic assumption if the ith measurement is obtained by time-averaging a sufficiently large number N of measurements made during smaller time intervals over which the biases $\{b_i(n)\}$ can be assumed constant. In this case, b_i will contain the mean of the biases $\{b_i(n)\}$ and the zero-mean noise ϵ_i will contain the contribution of the second and higher statistics of the $\{b_i(n)\}$ (for more details, see, e.g., [12, 13]).

Based on this model, it was shown in [13] that the asymptotic (for large N) mean-square error matrix for the biased estimation vector $\mathbf{x}_b$ can be written as

$$\mathrm{MSE}(\hat{\mathbf{x}}_b) = (\mathbf{H}\Sigma_\eta^{-1}\mathbf{H}^T)^{-1} + \mathbf{b}_x\mathbf{b}_x^T \tag{12}$$

$$\mathbf{b}_x = (\mathbf{H}\Sigma_\eta^{-1}\mathbf{H}^T)^{-1}\mathbf{H}\Sigma_\eta^{-1}\mathbf{b} \tag{13}$$

where for notation simplicity we defined $\Sigma_\eta \stackrel{\mathrm{def}}{=} \mathrm{CRLB}(\boldsymbol{\eta})$ and $\mathbf{b} = [b_1, b_2, \cdots, b_M]^T$ is the vector of measurement biases corresponding to the measurement vector $\boldsymbol{\eta} = [\eta_1, \eta_2, \cdots, \eta_M]^T$.

Note that while the first term in the right-hand side of (12) is equivalent to the CRLB matrix for the estimation of the MS's position in the absence of biased measurements (see (5)), the second term represents the nuisance effects of biased measurement errors.

Relationship with the GDOP matrix

In the GNSS literature, the matrix $\mathbf{H}$ as defined in (4) is called the geometry matrix and the $(\mathbf{H}\mathbf{H}^T)^{-1}$ matrix is called the geometric dilution of matrix (GDOP). It is the matrix of multipliers of ranging variance to give position variance [14]. For example, assuming that the covariance matrix of pseudo-range measurements is $\sigma_R^2\mathbf{I}$, the covariance matrix for the estimation vector $\mathbf{x} = [u_x, u_y, u_z, t_s]$ can be written using the GDOP matrix as

$$\mathrm{cov}(\mathbf{x}) = \sigma_R^2(\mathbf{H}\mathbf{H}^T)^{-1} \tag{14}$$

and the 4-diagonal elements of $(\mathbf{H}\mathbf{H}^T)^{-1}$ can be used to define other DOP metrics, such as the horizontal DOP (the square root of the sum of the first two terms) or the time DOP (the square root of the last term). For an arbitrary pseudo-range covariance matrix $\mathbf{Q}$, (14) can be written as

$$\mathrm{cov}(\mathbf{x}) = \left(\mathbf{H}\mathbf{Q}^{-1}\mathbf{H}^T\right)^{-1} \tag{15}$$

which is equivalent to the CRLB for $\mathbf{x}$ (see (3)), assuming that the pseudo-range measurement errors are Gaussian distributed [9].

Observation 5 *defining* $\mathbf{H}' = \sqrt{\gamma}\mathbf{H}$*, we obtain after replacing* $\mathbf{H}$ *with* $\mathbf{H}'$ *in (12)-(13) that* $\mathrm{MSE}'(\hat{\mathbf{x}}_b) = \frac{1}{\gamma}\mathrm{MSE}(\hat{\mathbf{x}}_b)$*. Thus, if the system geometry can be improved such as to reduce the product* $\mathbf{H}\mathbf{H}^T$ *by a scalar factor* γ*, the position MSE (or the CRLB and the bias term in (12)-(13)) will be reduced by a factor* γ*. however, it should be noted that reducing the covariance matrix* Σ_η *by a factor* γ *will only reduce the CRLB term on the right-hand side of (12), while the bias term will remain unchanged.*

Expressions for the matrix H

By defining the azimuth (measured clockwise from the Y direction) and elevation angles (measured up from local horizontal) between the MS's position $\mathbf{u}$ and the jth satellite or BS's position $\mathbf{p}_v^j$ as α_v^j and ϵ_v^j, respectively (see Fig. 2), and using (1) and (4), we obtain

$$(\mathbf{H})(i,j) = \begin{cases} \frac{u_x - p_{v,x}^j}{\|\mathbf{u}-\mathbf{p}_v^j\|} = \cos\epsilon_v^j \sin\alpha_v^j & , i=1 \\ \frac{u_y - p_{v,y}^j}{\|\mathbf{u}-\mathbf{p}_v^j\|} = \cos\epsilon_v^j \cos\alpha_v^j & , i=2 \\ \frac{u_z - p_{v,z}^j}{\|\mathbf{u}-\mathbf{p}_v^j\|} = \sin\epsilon_v^j & , i=3 \\ 1 & , i=4 \end{cases} . \tag{16}$$

Note that if the jth measurement is a range measurement, i.e., if the MS is time-synchronized and the jth measurement is obtained by subtracting the time of transmission from the time of arrival, then $t_s = 0$ in (1) and $(\mathbf{H})(4,j) = 0$ in (16). Consequently, if we consider a hybrid radio location system using S pseudo-range measurements and C range measurements, i.e., $\boldsymbol{\eta} = [\eta_1, \cdots, \eta_S, \eta_1, \cdots, \eta_C]$, the matrix $\mathbf{H}$ can be written in compact form as

$$\begin{aligned} \mathbf{H} &= \left[\begin{array}{ccc|ccc} \mathbf{b}_s^1 & \cdots & \mathbf{b}_s^S & \mathbf{b}_c^1 & \cdots & \mathbf{b}_c^C \\ \hline 1 & \cdots & 1 & 0 & \cdots & 0 \end{array}\right] \\ &\stackrel{\text{def}}{=} \left[\begin{array}{c|c} \mathbf{B}_s & \mathbf{B}_c \\ \hline \mathbf{1}^T & \mathbf{0}^T \end{array}\right] \end{aligned} \tag{17}$$

where the ith vector $\mathbf{b}_v^i$, $v \in \{s, c\}$ is defined as (see Fig. 2)

$$\mathbf{b}_v^i = [\cos\epsilon_v^i \sin\alpha_v^i, \cos\epsilon_v^i \cos\alpha_v^i, \sin\epsilon_v^i]^T. \tag{18}$$

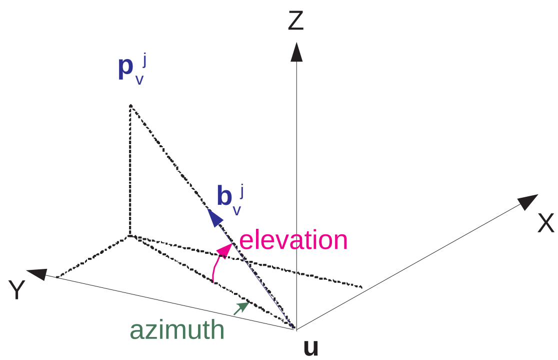

Fig. 2 Relationship between cartesian coordinates and azimuth and elevation.

ANALYTICAL RESULTS

In this section, we consider an hybrid system using time aiding information and analyze analytically the influence of the variance of the zero-mean clock error $\sigma_{t_s}^2$. For mathematical simplicity, we assume that $\boldsymbol{\eta}$ contains M independent identically distributed (i.i.d.) pseudo-range measurements, i.e., that we can write the CRLB for $\boldsymbol{\eta}$ as $\mathrm{CRLB}(\boldsymbol{\eta}) = \frac{1}{\sigma_s^2}\mathbf{I}$.

Using the above assumption together with (5), (7), (9), and (17), we obtain

$$\begin{aligned} \mathbf{J}_T(\mathbf{x}) &= \underbrace{\frac{1}{\sigma_s^2}\left[\begin{array}{c|c} \mathbf{B}_s\mathbf{B}_s^T & \mathbf{B}_s\mathbf{1} \\ \hline \mathbf{1}^T\mathbf{B}_s^T & M \end{array}\right]}_{\mathbf{J}_D(\mathbf{x})} + \underbrace{\mathrm{diag}\{0,0,0,1/\sigma_{t_s}^2\}}_{\mathbf{J}_P(\mathbf{x})} \\ &= \left[\begin{array}{c|c} \frac{1}{\sigma_s^2}\mathbf{B}_s\mathbf{B}_s^T & \frac{1}{\sigma_s^2}\mathbf{B}_s\mathbf{1} \\ \hline \frac{1}{\sigma_s^2}\mathbf{1}^T\mathbf{B}_s^T & \frac{M}{\sigma_s^2} + \frac{1}{\sigma_{t_s}^2} \end{array}\right]. \end{aligned} \tag{19}$$

By using the formulas for the inverse of a partitioned matrix (see, e.g., [5]), we can write the inverse FIM $\mathbf{J}_T^{-1}(\mathbf{x})$ as (only the diagonal elements are of interest)

$$\mathbf{J}_T^{-1}(\mathbf{x}) = \left[\begin{array}{c|c} \Phi_{xyz} & \cdot \\ \hline \cdot & \Phi_t \end{array}\right] \tag{20}$$

where

$$\Phi_{xyz}^{-1} = \mathbf{B}_s\left(\frac{1}{\sigma_s^2}\mathbf{I} - \frac{\frac{1}{\sigma_s^4}\mathbf{1}\mathbf{1}^T}{\frac{M}{\sigma_s^2} + \frac{1}{\sigma_{t_s}^2}}\right)\mathbf{B}_s^T \tag{21}$$

and

$$\Phi_t^{-1} = \frac{1}{\sigma_{t_s}^2} \tag{22}$$

In order to investigate the influence of the variance $\sigma_{t_s}^2$ of the GNSS time clock error t_s, we now consider the following two cases:

Case 1 : $\sigma_{t_s}^2 \ll \sigma_s^2/M$. The clock variance is assumed to be very small as compared to the variance of the pseudo-range measurements. Using the approximation $1/(1+x) \approx 1 - x$ valid for $|\,x\,| \ll 1$, we can write

$$\Phi_{xyz}^{-1} = \frac{1}{\sigma_s^2}\mathbf{B}_s\mathbf{B}_s^T - \mathbf{B}_s\mathbf{1}\mathbf{1}^T\mathbf{B}_s^T\frac{1}{M\sigma_s^2}\left\{\frac{M\sigma_{t_s}^2}{\sigma_s^2}\left(1 - \frac{M\sigma_{t_s}^2}{\sigma_s^2}\right)\right\}. \tag{23}$$

Consequently, we have

$$\lim_{M\sigma_{t_s}^2/\sigma_s^2 \to 0} \Phi_{xyz}^{-1} = \frac{1}{\sigma_s^2}\mathbf{B}_s\mathbf{B}_s^T \quad (24)$$

i.e., with very good prior knowledge of the clock, the second term in (23) vanishes and Φ_{xyz} converges towards the CRLB for range only estimation.

Case 2: $\sigma_{t_s}^2 \gg \sigma_s^2/M$. The clock variance is assumed large as compared to the variance of the pseudo-range measurements. Using the same approximation $1/(1+x) \approx 1-x$ valid for $| x | \ll 1$, we obtain

$$\Phi_{xyz}^{-1} = \frac{1}{\sigma_s^2}\mathbf{B}_s\mathbf{B}_s^T - \mathbf{B}_s\mathbf{1}\mathbf{1}^T\mathbf{B}_s^T\frac{1}{M\sigma_s^2}\left(1-\frac{\sigma_s^2}{M\sigma_t^2}\right). \quad (25)$$

Consequently, we have

$$\lim_{\sigma_s^2/(M\sigma_t^2)\to 0} \Phi_{xyz}^{-1} = \frac{1}{\sigma_s^2}\mathbf{B}_s\mathbf{B}_s^T - \mathbf{B}_s\mathbf{1}\mathbf{1}^T\mathbf{B}_s^T\frac{1}{M\sigma_s^2} \quad (26)$$

i.e., with very bad prior knowledge of the clock, the second term on the right-hand side of (25) converges towards $\mathbf{B}_s\mathbf{1}\mathbf{1}^T\mathbf{B}_s^T\frac{1}{M\sigma_s^2}$ and Φ_{xyz} converges towards the CRLB for pseudo-range estimation without prior knowledge of $\sigma_{t_s}^2$. In this case, the FIM $\mathbf{J}_T(\mathbf{x})$ may be (near-)singular if only 3 pseudo-range measurements are considered.

Observation 6 *comparing the right-hand side of (24) corresponding to the inverse CRLB matrix for* $\mathbf{x}$ *with range measurements with the right-hand side of (26) corresponding to the inverse CRLB matrix for* $\mathbf{x}$ *with pseudo-range measurements, we note that the CRLB for* $\mathbf{x}$ *assuming range measurements will always be smaller (or equal if* $\mathbf{B}_s\mathbf{1}\mathbf{1}^T\mathbf{B}_s^T = 0$*) than the CRLB for* $\mathbf{x}$ *assuming pseudo-range measurements (see also [5] where it is shown that an augmentation of the nuisance parameters can only result in an increase of the corresponding CRLB). Thus, a system of pseudo-range measurements for which the clock bias is unknown will always provide a worst (or at the best case equal) positioning accuracy than a system of range measurements (assuming the same system geometry).*

Observation 7 *if* $\mathbf{B}_s\mathbf{1}\mathbf{1}^T\mathbf{B}_s^T = 0$*, then we see by comparing the right hand sides of (24) and (26) that a system of pseudo-range measurements is equivalent to a system of range measurements (for the same system geometry). As shown in [9] and [15], this case only happens when the average LOS vector* $\bar{\mathbf{b}} = \sum_{i=1}^{S}\mathbf{b}_s = 0$ *(since we can write* $\mathbf{B}_s\mathbf{1}\mathbf{1}^T\mathbf{B}_s^T = \sum_{i=1}^{S}\frac{1}{\sigma_s^2}(\mathbf{b}_s^i - \bar{\mathbf{b}}_s)(\mathbf{b}_s^i - \bar{\mathbf{b}}_s)^T$*). Note that with satellite signals, this case does not happen as the overhead satellite components do not cancel.*

Observation 8 *for an hybrid system using S pseudo-range and C range measurements where* $\mathrm{CRLB}(\boldsymbol{\eta}_s) = \frac{1}{\sigma_s^2}\mathbf{I}$ *and* $\mathrm{CRLB}(\boldsymbol{\eta}_c) = \frac{1}{\sigma_c^2}\mathbf{I}$*, it is straightforward to show that* Φ_{xyz}^{-1} *as defined in (20) will contain the positive definite contributions due to the S pseudo-range measurements and the C range measurements, i.e.,*

$$\Phi_{xyz}^{-1} = \underbrace{\frac{1}{\sigma_s^2}\mathbf{B}_s\mathbf{B}_s^T - \mathbf{B}_s\mathbf{1}\mathbf{1}^T\mathbf{B}_s^T\frac{1}{S\sigma_s^2}}_{\text{pseudo-range contribution}} + \underbrace{\frac{1}{\sigma_c^2}\mathbf{B}_c\mathbf{B}_c^T}_{\text{range contribution}}. \quad (27)$$

Consequently, the CRLB for a hybrid system using both range and pseudo-range measurements will always be smaller than for a system using range or pseudo-range individually.

NUMERICAL RESULTS

In this section, we present Monte-Carlo simulation results for the hybrid configurations C1-C11, obtained using the CRLB and asymptotic MSE expressions developed in the previous sections. Assuming unbiased or biased cellular pseudo-ranges, we compute the horizontal distance rms as $DRMSE_{CRLB} = \sqrt{\mathrm{CRLB}(u_x)+\mathrm{CRLB}(u_y)}$ or $\mathrm{DRMSE}_{MSE} = \sqrt{\mathrm{MSE}(u_x)+\mathrm{MSE}(u_y)}$, respectively. We assume the following conditions:

- GNSS positions: a total of 288 satellite GPS constellations are simulated (every 5 minutes for 24 hours) using the interactive GPS satellite prediction utility (see: [16]). The simulations are for August 11, 2004 starting at 00:00:00 UTC (GPS week = 256 GPS TOW = 259200 seconds), Altitude = 500.0 meters, Latitude = 46 59'37.78"N, Longitude = 6 56' 25.53"E (corresponding to our laboratory's position), using an elevation mask of 49^o. Table. 1 presents the percentage of satellites that were visible simultaneously during the 24 hour simulation period.

- BSs positions: three BSs at zero degree elevation and forming an equilateral triangle with a base of 5 km are assumed.

- MS position: the MS's position is assumed to be uniform on a circle of radius $5 \times \sqrt{3}/6$ and centered within the positions of the three BSs.

- Error biases and error p.d.f.s: because in urban canyons, the MS may still have LOS with a few satellites (at high elevation angles) but will not in general have LOS with the cellular BSs (at near-zero elevation angles), we consider unbiased satellite pseudo-range measurements and biased cellular pseudo-range measurements. In order to generalize the results we obtain, we assume that the satellite pseudo-ranges are zero mean Gaussian distributed with a standard deviation σ_o, and express all the other standard deviations as a function of σ_o. In this way, it is possible to generalize the results we obtain for any standard deviation σ_o. The different p.d.f.s we assume are summarized in Table 2. Note that a practical value for σ_o is typically 5.3 m for a civilian GPS C/A receiver without selective availability [14, p.451].

In addition to the DRMSE metrics described above and in order to get a feeling about the impact of each hybrid GNSS/cellular method on the system geometry, we computed

Table 1 Percentage of satellites that were visible simultaneously during the 24 hours simulation period.

# Satellites	Percentage
1	7.65
2	43.1
3	41.6
4	7.65
> 4	0

Table 2 Probability density functions for the pseudo-ranges, pseudo-range biases, time aiding information, and altitude aiding information.

Parameter	Probability density function
Satellites PRs	$N[0, \sigma_o^2]$
BS PRs	$N[0, (\gamma_{PR}\sigma_o)^2]$, $\gamma_{PR} \in \{1, 5, 10\}$
Time aiding	$N[0, (\gamma_{t_s}\sigma_o)^2]$, $\gamma_{t_s} \in \{1, 5, 10\}$
Altitude aid.	$N[0, (\gamma_{u_z}\sigma_o)^2]$, $\gamma_{u_z} \in \{1, 5, 10\}$
BS biases	$U[0, (\gamma_{BIAS}\sigma_o)^2]$, $\gamma_{BIAS} \in \{0, 20, 50\}$

the horizontal dilution of precision (HDOP) metric (i.e., for every Monte-Carlo simulation, we calculated the square-root of the sum of the first two diagonal elements of the matrix $(\mathbf{H}\mathbf{H}^T)^{-1}$). Note that with altitude and time aiding information, the third and forth row of the matrix $\mathbf{H}$, respectively, was removed, which corresponds to assume no error in the data aiding information.

For each hybrid GNSS/cellular configuration and each of the 288 simulated satellite constellations, we used 500 Monte-Carlo simulations to average the CRLB and MSE results over the random error distributions and MS's positions. Table 3–5 show the threshold values $\{X\}$, for which the probability that $\text{HDOP} \leq X$ or $\text{DRMSE} \leq X$ is p, for $p \in \{0.67, 0.90, 0.95\}$.

Discussion

From Table 3, we make the following observations:

- The overall HDOP for the simulated MS's positions and time period was relatively large (the HDOP for 4 satellites was only below 6.5 during 67% of the 24-hour period).
- With 3 satellites, time aiding information produces a slightly better HDOP than altitude aiding information (see cases C3-C4).
- The lowest HDOP is obtained for the hybrid cases using 3 cellular terrestrial measurements. It can be shown that the minimum HDOP is $2/\sqrt{C}$ when C BSs are placed on a C-sided regular polygon [17] (for 3 BSs, the minimum HDOP is thus $2/\sqrt{3} \approx 1.155$ with the MS at the center of the polygon).

From Table 4, we make the following observations:

- The contribution to accuracy of the cellular PR measurements can be severely degraded when the cellular PR measurements are corrupted with important biases. For example, comparing case C1 with cases C3-C4, we note that for $\gamma_{BIAS} = 0$, the accuracy is better when using 3 satellite PRs and 1 cellular PR than when using 3 satellite PRs and time or altitude aiding information. However, for the more realistic cases when $\gamma_{BIAS} \in \{20, 50\}$, the accuracy obtained with 3 satellite PRs and time or altitude aiding information is often significantly better (recall that NLOS propagation does not impact the RTD-based time aiding estimation given reciprocity of propagation times on the forward and reverse link).
- In addition to providing a better accuracy in important terrestrial NLOS conditions, it should be noted that another advantage of using altitude aiding information versus a cellular PR measurement is that the cellular BS does not need to be GNSS time-synchronized.
- Comparing case C3 with C2, we note that the addition of a moderately biased cellular PR measurement ($\gamma_{BIAS} \in \{0, 20\}$) improves the accuracy. However, the addition of an importantly biased cellular PR measurement ($\gamma_{BIAS} = 50$) degrades the accuracy.
- The accuracy that can be achieved using time aiding information is superior to the one achieved with altitude aiding information (see case C3 and C4). This can be explained by noting in Table 3 that the HDOP is smaller for time aiding information than for altitude aiding information. Of course, as illustrated in case C5, the accuracy is even better when both time and altitude aiding information are used together.

From Table 5, we make the following observations:

- The accuracy when using only two satellite PRs and two cellular measurements (see cases C7 and C8) is worst than when using 3 satellite PRs and one BS measurement (see Table 4). The difference is even more pronounced for important biased cellular measurements.
- The worst accuracy is obtained for the case C9, i.e., when only the time and altitude aiding information of a single MS is used together with 2 satellite PR measurements. In fact, comparing case C9 with case C10, we note that trading an unbiased satellite PR measurement with an additional biased cellular PR measurement can improve significantly the DRMSE accuracy by making the HDOP becoming much smaller (see also Table 3).
- Comparing case C7 with C8 or case C10 with C11, we note that, as expected, the addition of time aiding information to 4 cellular and satellite PR measurements improves the positioning accuracy.
- For moderately biased cellular PR measurements ($\gamma_{BIAS} = 20$, $\gamma_{PR} = 5$), the accuracy using a single satellite PR measurement and 3 BS measurements is

Table 3 Threshold X in m for which $prob(HDOP \leq X) = p$, $p \in \{0.67, 0.90, 0.95\}$

Hybrid cases	Threshold X in meters for p=0.67	p=0.90	p=0.95
C1) 3 SAT$_{3PR}$ + 1 BS$_{PR}$	7.4	24.9	41.5
C2) 3 SAT$_{3PR}$ + 1 BS$_{RTD+PR}$	2.5	3.9	5.2
C3) 3 SAT$_{3PR}$ + 1 BS$_{RTD}$	7.5	22.3	56.8
C4) 3 SAT$_{3PR}$ + 1 BS$_{ALT}$	8.0	34.5	88.0
C5) 3 SAT$_{3PR}$ + 1 BS$_{RTD+ALT}$	4.9	6.9	9.8
C6) 4 SAT$_{4PR}$	6.5	12.3	21.4
C7) 2 SAT$_{2PR}$ + 2 BS$_{2PR}$	3.5	16.9	33.4
C8) 2 SAT$_{2PR}$ + 2 BS$_{RTD+2PR}$	1.8	3.0	4.6
C9) 2 SAT$_{2PR}$ + 1 BS$_{RTD+ALT}$	14.9	35.9	59.4
C10) 1 SAT$_{PR}$ + 3 BS$_{3PR}$	1.4	1.4	1.4
C11) 1 SAT$_{PR}$ + 3 BS$_{RTD+3PR}$	1.3	1.3	1.3

Table 4 Normalized threshold X in m for which $prob(\text{DRMSE} \leq X) = p$, $p \in \{0.67, 0.90, 0.95\}$

Parameters					Threshold X in meters for		
Hybrid cases with 3 sat.	γ_{PR}	γ_{t_s}	γ_{u_z}	γ_{BIAS}	p=0.67	p=0.90	p=0.95
C1) 3 SAT$_{3PR}$ + 1 BS$_{PR}$	01	N/A	N/A	00	6.7	21.4	39.9
C1) 3 SAT$_{3PR}$ + 1 BS$_{PR}$	05	N/A	N/A	00	7.3	23.2	42.9
C1) 3 SAT$_{3PR}$ + 1 BS$_{PR}$	10	N/A	N/A	00	8.7	27.2	49.5
C1) 3 SAT$_{3PR}$ + 1 BS$_{PR}$	01	N/A	N/A	20	9.3	29.3	53.8
C1) 3 SAT$_{3PR}$ + 1 BS$_{PR}$	05	N/A	N/A	20	9.7	30.6	56.0
C1) 3 SAT$_{3PR}$ + 1 BS$_{PR}$	10	N/A	N/A	20	10.7	33.7	60.8
C1) 3 SAT$_{3PR}$ + 1 BS$_{PR}$	01	N/A	N/A	50	16.1	48.6	92.0
C1) 3 SAT$_{3PR}$ + 1 BS$_{PR}$	05	N/A	N/A	50	16.3	49.4	93.4
C1) 3 SAT$_{3PR}$ + 1 BS$_{PR}$	10	N/A	N/A	50	16.9	51.9	97.5
C2) 3 SAT$_{3PR}$ + 1 BS$_{RTD+PR}$	01	01	N/A	00	2.4	3.9	5.1
C2) 3 SAT$_{3PR}$ + 1 BS$_{RTD+PR}$	05	05	N/A	00	5.3	8.2	10.2
C2) 3 SAT$_{3PR}$ + 1 BS$_{RTD+PR}$	10	10	N/A	00	7.0	12.8	16.3
C2) 3 SAT$_{3PR}$ + 1 BS$_{RTD+PR}$	01	01	N/A	20	6.1	16.0	29.5
C2) 3 SAT$_{3PR}$ + 1 BS$_{RTD+PR}$	05	05	N/A	20	7.8	18.1	30.8
C2) 3 SAT$_{3PR}$ + 1 BS$_{RTD+PR}$	10	10	N/A	20	9.2	21.8	34.6
C2) 3 SAT$_{3PR}$ + 1 BS$_{RTD+PR}$	01	01	N/A	50	13.2	39.2	73.5
C2) 3 SAT$_{3PR}$ + 1 BS$_{RTD+PR}$	05	05	N/A	50	14.2	39.8	73.9
C2) 3 SAT$_{3PR}$ + 1 BS$_{RTD+PR}$	10	10	N/A	50	15.3	41.5	74.9
C3) 3 SAT$_{3PR}$ + 1 BS$_{RTD}$	N/A	01	N/A	00	6.9	22.0	50.2
C3) 3 SAT$_{3PR}$ + 1 BS$_{RTD}$	N/A	05	N/A	00	7.7	24.5	54.8
C3) 3 SAT$_{3PR}$ + 1 BS$_{RTD}$	N/A	10	N/A	00	9.1	32.0	64.7
C4) 3 SAT$_{3PR}$ + 1BS$_{ALT}$	N/A	N/A	01	00	7.3	29.9	69.9
C4) 3 SAT$_{3PR}$ + 1BS$_{ALT}$	N/A	N/A	05	00	7.9	33.5	80.5
C4) 3 SAT$_{3PR}$ + 1BS$_{ALT}$	N/A	N/A	10	00	9.2	40.9	97.8
C5) 3 SAT$_{3PR}$ + 1BS$_{RTD+ALT}$	N/A	01	01	00	5.7	11.6	16.4
C5) 3 SAT$_{3PR}$ + 1BS$_{RTD+ALT}$	N/A	05	05	00	7.4	21.4	39.2
C5) 3 SAT$_{3PR}$ + 1BS$_{RTD+ALT}$	N/A	10	10	00	8.3	29.2	56.0

Table 5 Normalized threshold X in m for which $prob(\text{DRMSE} \leq X) = p$, $p \in \{0.67, 0.90, 0.95\}$

Parameters					Threshold X in meters for		
Hybrid cases with 1,2,4 sat.	γ_{PR}	γ_{t_s}	γ_{u_z}	γ_{BIAS}	p=0.67	p=0.90	p=0.95
C6) 4 SAT$_{4PR}$	N/A	N/A	N/A	00	6.7	12.8	21.1
C7) 2 SAT$_{2PR}$ + 2 BS$_{2PR}$	01	N/A	N/A	00	3.7	14.4	29.5
C7) 2 SAT$_{2PR}$ + 2 BS$_{2PR}$	05	N/A	N/A	00	8.2	28.9	54.6
C7) 2 SAT$_{2PR}$ + 2 BS$_{2PR}$	10	N/A	N/A	00	15.3	49.9	93.3
C7) 2 SAT$_{2PR}$ + 2 BS$_{2PR}$	01	N/A	N/A	20	9.6	33.2	63.3
C7) 2 SAT$_{2PR}$ + 2 BS$_{2PR}$	05	N/A	N/A	20	12.1	42.6	79.3
C7) 2 SAT$_{2PR}$ + 2 BS$_{2PR}$	10	N/A	N/A	20	17.7	60.1	111.3
C7) 2 SAT$_{2PR}$ + 2 BS$_{2PR}$	01	N/A	N/A	50	22.1	68.9	134.9
C7) 2 SAT$_{2PR}$ + 2 BS$_{2PR}$	05	N/A	N/A	50	23.7	75.3	145.7
C7) 2 SAT$_{2PR}$ + 2 BS$_{2PR}$	10	N/A	N/A	50	27.2	88.9	168.7
C8) 2 SAT$_{2PR}$ + 2 BS$_{RTD+2PR}$	01	01	N/A	00	2.1	3.6	5.6
C8) 2 SAT$_{2PR}$ + 2 BS$_{RTD+2PR}$	05	05	N/A	00	6.6	10.7	16.5
C8) 2 SAT$_{2PR}$ + 2 BS$_{RTD+2PR}$	10	10	N/A	00	12.3	20.4	29.7
C8) 2 SAT$_{2PR}$ + 2 BS$_{RTD+2PR}$	01	01	N/A	20	8.9	27.1	52.6
C8) 2 SAT$_{2PR}$ + 2 BS$_{RTD+2PR}$	05	05	N/A	20	10.9	30.8	56.7
C8) 2 SAT$_{2PR}$ + 2 BS$_{RTD+2PR}$	10	10	N/A	20	15.3	37.6	65.6
C8) 2 SAT$_{2PR}$ + 2 BS$_{RTD+2PR}$	01	01	N/A	50	21.5	65.3	128.6
C8) 2 SAT$_{2PR}$ + 2 BS$_{RTD+2PR}$	05	05	N/A	50	22.5	67.3	130.4
C8) 2 SAT$_{2PR}$ + 2 BS$_{RTD+2PR}$	10	10	N/A	50	24.9	71.2	134.7
C9) 2 SAT$_{2PR}$ + 1 BS$_{RTD+ALT}$	N/A	01	01	00	27.3	68.0	135.3
C9) 2 SAT$_{2PR}$ + 1 BS$_{RTD+ALT}$	N/A	05	05	00	120.7	272.6	519.5
C9) 2 SAT$_{2PR}$ + 1 BS$_{RTD+ALT}$	N/A	10	10	00	240.8	541.6	1030.7
C10) 1 SAT$_{PR}$ + 3 BS$_{3PR}$	01	N/A	N/A	00	1.4	2.0	2.2
C10) 1 SAT$_{PR}$ + 3 BS$_{3PR}$	05	N/A	N/A	00	7.2	9.8	11.1
C10) 1 SAT$_{PR}$ + 3 BS$_{3PR}$	10	N/A	N/A	00	14.4	19.6	22.1
C10) 1 SAT$_{PR}$ + 3 BS$_{3PR}$	01	N/A	N/A	20	8.6	11.9	13.2
C10) 1 SAT$_{PR}$ + 3 BS$_{3PR}$	05	N/A	N/A	20	11.2	14.1	15.4
C10) 1 SAT$_{PR}$ + 3 BS$_{3PR}$	10	N/A	N/A	20	16.6	21.4	23.6
C10) 1 SAT$_{PR}$ + 3 BS$_{3PR}$	01	N/A	N/A	50	21.2	29.5	32.9
C10) 1 SAT$_{PR}$ + 3 BS$_{3PR}$	05	N/A	N/A	50	22.3	30.3	33.6
C10) 1 SAT$_{PR}$ + 3 BS$_{3PR}$	10	N/A	N/A	50	25.6	33.1	36.1
C11)1 SAT$_{PR}$ + 3 BS$_{RTD+3PR}$	01	01	N/A	00	1.3	1.8	2.1
C11)1 SAT$_{PR}$ + 3 BS$_{RTD+3PR}$	05	05	N/A	00	6.6	9.0	10.3
C11)1 SAT$_{PR}$ + 3 BS$_{RTD+3PR}$	10	10	N/A	00	13.1	18.0	20.5
C11)1 SAT$_{PR}$ + 3 BS$_{RTD+3PR}$	01	01	N/A	20	8.6	11.9	13.2
C11)1 SAT$_{PR}$ + 3 BS$_{RTD+3PR}$	05	05	N/A	20	10.8	13.7	15.1
C11)1 SAT$_{PR}$ + 3 BS$_{RTD+3PR}$	10	10	N/A	20	15.6	20.0	22.2
C11)1 SAT$_{PR}$ + 3 BS$_{RTD+3PR}$	01	01	N/A	50	21.2	29.5	32.9
C11)1 SAT$_{PR}$ + 3 BS$_{RTD+3PR}$	05	05	N/A	50	22.2	30.2	33.5
C11)1 SAT$_{PR}$ + 3 BS$_{RTD+3PR}$	10	10	N/A	50	25.0	32.5	35.6

on the same order of magnitude as the accuracy using 4 satellite PR measurements (see cases C10-C11 and C6). However, if the cellular biases are important, the 4 satellite PRs will provide a better positioning accuracy, as the lower HDOP will not compensate anymore for the large biased cellular measurements.

CONCLUSIONS

In this paper, we have presented a mathematical framework to study the achievable positioning performance of hybrid GNSS/cellular systems. Contrarily to the DOP metrics, this framework can be used to provide insights into the influence of uncertainties in the data aiding information (such as time and altitude aiding information), and biases in the pseudorange measurements.

Using Monte-Carlo simulations for a particular cellular and system geometry, we observed that time aiding information based on a cellular RTD measurement can provide a much improved positioning accuracy than a cellular PR measurement. This is because NLOS propagation can result in important biased cellular PR measurements while the RTD-based time aiding information is independent of NLOS (given reciprocity of propagation times on the forward and reverse link). It is also observed that a missing satellite PR measurement can easily be replaced with a cellular measurement without affecting too much the positioning accuracy. Similarly, a single unbiased satellite measurement in addition to 3 biased cellular PR measurements can also provide a good positioning accuracy as the very small HDOP obtained with the 3 cellular BSs and one satellite compensates for the biases of the cellular PR measurements. However, this is not the case when two satellite and two cellular PR measurements are used as the two cellular biased measurements are not compensated anymore with a small HDOP and the DRMSE becomes very large.

Finally, we note that the mathematical framework we obtained could easily be extended to other form of measurements (such as angle of arrivals, etc.), and thus provides an additional design tool for the system engineers to investigate the positioning performance of hybrid GNSS/cellular systems under various conditions.

REFERENCES

[1] Heinrichs G., Eissfeller B., “Synergies on handset architecture level for combined gnss and wireless location,” in *ION GPS 2001*, 2001.

[2] Ma C., “Integration of GPS and cellular networks to improve wireless location performance,” in *ION GPS/GNSS 2003*, 2003, pp. 1585–1996.

[3] Son H., Lee J., Jee G., “Mobile station location using hybrid gps and a wireless network,” in *IEEE Vehicular Technology Conference, VTC 2003 - Spring*, apr 2003, vol. 4, pp. 2716–2720.

[4] Soliman, S, Agashe, P., Fernandez, I., Vayanos, A., Gaal, P., Oljaca, M., “gpsone^{TM}: a hybrid position location system,” in *IEEE Sixth International Symposium on Spread Spectrum Techniques and Applications*, sep 2000, vol. 1, pp. 330–335.

[5] Scharf L.L., *Statistical Signal Processing: Detection, Estimation, and Time Series Analysis,* Addison-Wesley, Reading, Massachusetts, 1991.

[6] Van Trees H.L., *Detection, Estimation, and Modulation Theory, Part I,* Wiley, New York, 1968.

[7] Chan Y.T., Ho K.C., “A simple and efficient estimator for hyperbolic location,” *IEEE Trans. Signal Processing*, vol. 42, no. 8, pp. 1905–1915, Aug. 1994.

[8] Reed C.W., Hudson R., Yao K., “Direct joint source localization and propagation speed estimation,” in *IEEE Int. Conf. on Acoustics, Speech, and Signal Processing: ICASSP 1999*, 1999, vol. 3, pp. 1169–1172.

[9] Chaffee J., Abel J., “GDOP and the Cramer-Rao bound,” in *IEEE Position Location and Navigation Symposium*, Apr. 1994, pp. 663–668.

[10] Wylie M.P., Holtzman J. , “The non-line of sight problem in mobile location estimation,” in *IEEE Int. Conf. on Universal Personal Communications*, Oct. 1996, vol. 2, pp. 827–831.

[11] Botteron C., Høst-Madsen A., Fattouche M., “Cramer-Rao bounds for the estimation of multipath parameters and mobiles’ positions in asynchronous DS-CDMA systems,” *IEEE Trans. Signal Processing*, vol. 52, no. 4, pp. 862–875, apr 2004.

[12] Koorapaty H., Grubeck H., Cedervall M., “Effect of biased measurement errors on accuracy of position location methods,” in *IEEE Global Telecommunications Conference, GLOBECOMM 1998*, 1998, vol. 3, pp. 1497–1502.

[13] Botteron C., Høst-Madsen A., Fattouche M., “Effects of system and environment parameters on the performance of network based mobile station position estimators,” *IEEE Trans. Veh. Technol.*, vol. 53, no. 1, pp. 163–180, Jan. 2004.

[14] Parkinson B.W., Spilker J.Jr., *Global Positioning System: Theory and Applications*, vol. 1 of *Progress in astronautics and aeronautics ; 163*, American Institute of Aeronautics and Astronautics, Inc., Washington, D.C., 1996.

[15] Abel J.S., Chaffee J.W., “Integrating GPS with ranging transponders,” in *ION National Technical Meeting*, Jan. 1991, pp. 15–24.

[16] *Interactive GPS Satellite Prediction Utility,* NAWCWPNS GPS/INS Section, `http://sirius.chinalake.navy.mil/satpred/`.

[17] Levanon N., “Lowest GDOP in 2-D scenarios,” *IEE Proc.-Radar, Sonar Navig.*, vol. 147, no. 3, pp. 149–155, jun 2000.